

Rewriting the Limits for Deep Geothermal Drilling: Direct Energy Drilling Using Millimeter Wave Technology

Matt Houde¹, Carlos Araque¹, Ken Oglesby², and Paul Woskov³

¹Quaise, Inc., 501 Massachusetts Ave., Cambridge, MA 02139; ²Impact Technologies LLC, P.O. Box 35505 Tulsa, OK 74153-0505; ³MIT Plasma Science and Fusion Center, NW16-110, 167 Albany St, Cambridge, MA 02139

¹matt@quaise.energy, ²kdo2@impact2u.com, ³ppwoskov@mit.edu

Keywords: Deep Drilling, Hot Dry Rock, EGS, Supercritical, Millimeter-Wave, Casing-While-Drilling.

ABSTRACT

Vast amounts of energy are stored as heat in dry rock. At depths ranging from 10-20 km, the temperature and pressure reach supercritical conditions where potential power output is increased significantly compared to conventional geothermal resources. Supercritical geothermal resources remain untapped, but what if innovations in drilling technology could provide access to supercritical conditions anywhere on earth and within 100 days? What if exploration risk would no longer be significant because the incremental costs of drilling deeper would be relatively small and geothermal power could be produced locally, near high-demand centers? This would forever change the outlook and scalability of geothermal energy as a compelling alternative for countries transitioning to clean energy, although mechanical drilling methods cannot penetrate these depths and are a mature technology only capable of incremental improvements.

Technical limitations to deep geothermal drilling could be overcome by direct energy drilling using Millimeter Wave (MMW) technology. Full bore penetration would be transformed into solely an energy-matter interaction, an entirely new approach that removes high temperature and high-pressure limits imposed on mechanical tools. MMW drilling has the potential to increase conventional drilling rates of penetration (ROP) by a factor of 10 or more, enable casing-while-drilling, and access depths up to 10-20 km. In this paper, we revisit the concept of direct-energy drilling via millimeter waves, pioneered at the MIT Plasma Science Fusion Center and now on active development at Quaise, Inc., to show the potential and feasibility of this technology both technically and economically. We use simple models to demonstrate likely rates of penetration, material removal techniques, casing-while-drilling and economic value, and outline a technology, product, and business development roadmap to get there at scale.

1. INTRODUCTION

The heat flux that continuously emanates through the earth's crust is estimated at about 5.4×10^{21} MJ (WEC, 2013). Compared to annual world energy consumption, 6.1×10^{14} MJ for 2015, extracting just 0.1% of this available energy would be enough to meet global energy demand for over a million years (EIA, 2017). Despite this enormous potential, only a small fraction of this heat content makes itself available as conventional geothermal energy, which is a rare occurrence outside of ideal locations near tectonic plate boundaries. Scaling up geothermal power to meet a significant portion of world energy demand requires development of Enhanced Geothermal Systems (EGS) technology. Decades of research have gone into the EGS concept but attempts at developing a commercial EGS power plant have met limited success and have not seen widespread adoption despite the resource potential. Recent efforts have been focused on exploiting low temperature geothermal resources, by increasing the flow rate with stimulation technologies derived from the Oil and Gas (O&G) industry. However, the number of wells required result in high drilling costs and the costs of materials alone could prove uneconomical. The ability to effectively enhance permeability for EGS in shallow crystalline rock is highly site dependent, so improved techniques may not prove scalable for widespread deployment (Lowry et al., 2017) (Jung, 2013).

An alternative approach is to increase the flow temperature past the critical point of water, where it will enter a supercritical state. At these temperatures, a geothermal well would generate an order of magnitude more energy compared to a conventional geothermal well, which could improve the economics for EGS to scale at any location (Friðleifsson et al., 2014). Efforts are already underway in several countries with experience in geothermal to tap into supercritical geothermal resources overlying shallow magma bodies where conventional geothermal is already exploited (Dobson et al., 2017). The economics become much more favorable for "supercritical EGS" if power production can be increased to negate the cost increase for drilling deeper wells.

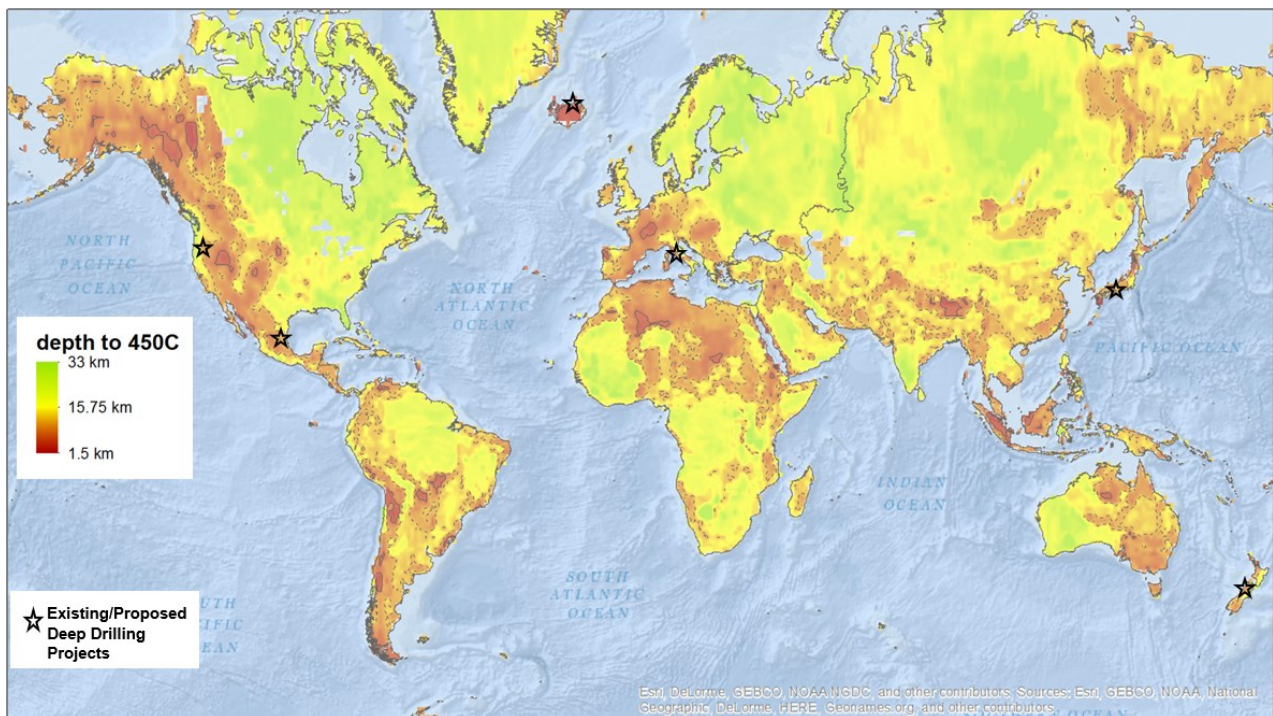


Figure 1: World contour map showing depths to 450 °C. Approximately 81% of the world’s population has access to supercritical conditions at <20 km depth, but few locations have a shallow heat source to reach supercritical temperatures at the shallow drilling depths that are currently economical (Claudohos et al., 2018).

Assuming an average geothermal gradient of 30 °C/km, supercritical temperatures can be reached for most of the world’s population at depths between 10–20 km (figure 1). Supercritical EGS requires disruptive innovation in two key technology areas: (1) *stimulation methods*, that scale to be consistently applicable across a wide range of geologic formations at depths near or at the Brittle-Ductile Transition (BDT); and (2) *cost-effective methods to drill deep* for economically attractive temperatures (Claudohos et al., 2018) (DOE Geovision, 2014). Supercritical EGS can accelerate geothermal beyond a niche source of energy for the world, but only if drilling technology is also advanced to make drilling depths of 10–20 km economic. New drilling techniques must improve the ROP by an order of magnitude and achieve a dramatic savings in casing cost to make supercritical EGS practical anywhere.

2. DEEP DRILLING CONSTRAINTS

Significant improvements in conventional drilling technology have been lacking, as mechanical drilling equipment face several shortcomings in drilling through high temperatures and hard abrasive rock. This includes degradation of mechanical equipment, low efficiency/Rate of Penetration (ROP), and significant time lost to tripping/fishing the drill string and other repairs to the mechanical assemblage (GEECO, 2011). The WellCost Lite model predicts well costs of \$2,000 - \$4,000/m are expected for a 5-km EGS well, so drilling costs could increase exponentially when attempting to reach supercritical conditions (Tester et al., 2006). In-situ conditions for supercritical EGS at most locations will be deep and hot enough to exceed the specifications for mechanical drilling tools – the deepest boreholes in the world have barely exceeded 12 km depth before high temperatures or other limitations were reached.

An innovative solution is directed energy drilling, which would replace mechanical rock destruction method with an energy-matter interaction: intense energy will melt/vaporize matter and create a propagation path through it, while also having the potential to replace casing/cementing with a durable vitrified liner produced along the borehole walls. Rock penetration would cease to be limited by rock hardness and temperature as no mechanical equipment would be required downhole. Directed energy drilling research has been conducted for over 5 decades, focused on lasers, but the longest penetration achieved to date has not eclipsed 60 cm (Gahan, 2005). Lasers are inefficient (<10%) at high power and their short wavelengths are fundamentally incompatible with the rock extraction particle flow for long distance transmission through deep boreholes (Nusinovich et al., 2014). An alternative approach is increase to an optimal wavelength for electromagnetic radiation that can propagate more efficiently over large distances and through small particulate filled propagation paths.

3. MILLIMETER-WAVE DRILLING

Electromagnetic (non-ionizing) radiation between 30 to 300 GHz has a wavelength of 1-mm to 10-mm, called Millimeter-Waves (MMW). At these longer wavelengths, electromagnetic radiation avoids Rayleigh scattering and can transfer energy 10^{12} times more efficiently through a fine particulate cloud than laser sources. High-powered sources of MMW are available via gyrotrons, a technology that has been around for over 50 years and developed as part of nuclear fusion research to heat plasmas. Gyrotrons are a class of free electron masers: a high-voltage electron beam is generated inside a strong magnetic field, causing electrons to gyrate around magnetic field lines, then efficiently convert the electron beam energy, through electron cyclotron resonance, into powerful radiation (Nusinovich, 2004). Gyrotrons are much more efficient (50%) than high-power lasers, and several MW-scale units are currently in use around the world for fusion research, such as the International Thermonuclear Experiment Reactor (Jacquinot, 1998). Rugged, transportable MW-scale gyrotron systems have been developed for use by the U.S. Department of Defense, so modest adaptation is required to modify this system for a drilling operation (Blank et al., 2008).

3.1 MMW Drilling Concept

The general concept for *MMW Drilling* is illustrated in figure 2 (Woskov & Cohn, 2009). High-powered MMW radiation is generated at the surface by a gyrotron and efficiently guided long distances by both metallic waveguides and the vitrified (glass formed by rock melt) borehole wall. The only downhole component required is the metallic waveguide (see figure 2), which serves as a conduit for MMW beam energy, purge gas flow, and remote diagnostics (US Patent #8393410B2, 2013). Rock will absorb the MMW beam, rapidly raising the surface temperature of the rock to over 3000 °C that will melt or vaporize the rock exposed, depending on power input and time of exposure (Hagen 1999). The waveguide is kept at a standoff distance from the melt/vaporization front as the MMW beam is launched, for survivability, and naturally diverges to ream a borehole diameter larger than the waveguide, leaving an annular space for debris removal or exhaust. MMW directed energy is delivered as a Gaussian beam, with less power absorbed along the borehole edge that will simultaneously vitrify the borehole wall to provide a liner seal that can stabilize the borehole after cooldown. The vitrified liner itself will act as a dielectric waveguide to continue propagation of energy to borehole bottom, which could enable very large standoff distances (> 100 m) between waveguide and vaporization/melting front.

Debris is either vaporized and evacuated up the borehole with the injected purge gas as a nano-particulate smoke: *Full Bore Vaporization*; or permeated into adjacent fractures as rock melt/particulate: *Partial Melt Displacement*. If vaporized, rock vapor will quench to form a nano-particulate “smoke”, which can be conveyed upward to the surface or blown out through adjacent fractures by the injected purge gas (Whitlock & Frick, 1994) (Hunten et al., 1980) (Zimmer 2002). If the borehole volume can be confined or restricted, the temperature increase should result in an equal increase in pressure according to the real gas law: this results in an overpressure condition downhole. The ideal gas law predicts that vaporizing rock could produce pressures up to 1000 MPa, higher than lithostatic pressures at 15 km (Woskov & Cohn, 2009). The ideal gas law is a good approximation of the real gas law for supercritical fluids at high temperatures considered here (Nordstrom & Munoz, 1994). Rock melt will have a low viscosity above 1500 °C, so the high pressures generated should be able to permeate the melt into in-situ micro fractures or fractures thermally induced by high temperature penetration (Nikolaevskiy & Garagash, 2004). This would lower the energy requirements to both destroy and extract the rock, as rock can be melted at a lower temperature and displaced downhole versus transporting the vaporized particulate products to the surface. Rock melt can also provide a thicker, stronger vitrified liner to serve as a replacement for casing.

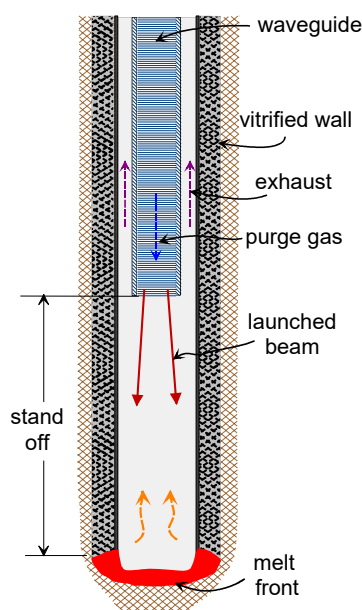


Figure 2: Downhole components of a MMW drilling system (vertical cross-section).

MMW drilling is proposed to replace the core functions of conventional drilling: (1) rock destruction, (2) debris removal, and (3) borehole stabilization. A mechanical drilling rig fulfills these tasks with a bottom hole assembly of drill bit + string, drilling mud, and other mechanical tools. MMW drilling will replace all three functions with a directed energy drilling operation: intense energy will melt/vaporize rock at high temperatures that generates an overpressure condition inside the borehole, conveying debris up-hole or into adjacent fractures for removal while stabilizing the borehole until a competent vitrified liner is produced along the borehole wall to permanently seal and support the open hole. The overpressure condition will control and prevent influx to maintain control of the well for personnel safety and public environmental protection. Rock hardness and temperature will no longer limit drilling capabilities and could make rock destruction easier at higher temperatures due to greater influence of thermal stresses. ROP could increase ten-fold, and the potential for casing-while-drilling would remove casing costs from the total well costs.

3.2 MMW Drilling System Components

A system schematic for the “MMW Drilling Rig” is shown in figure 3. Just under 50% of energy goes toward powering the gyrotron; the remaining power goes toward purge gas injection, waveguide handling, and remote diagnostics. The purge system will incorporate high-powered compressors that inject pressurized purge gas at the wellhead manifold, to deliver gas injection concurrent with the MMW beam for debris removal. Air or nitrogen is suitable for testing at shallow depths, but eventually an inert gas such as argon will be required because the purge gas must be transparent to MMW at high pressures, where fluid is expected to become supercritical. This parameter space is unexplored and unforeseen approaches to borehole stabilization might become possible with directed energy drilling. Some power is also required for waveguide mechanical movement (i.e. lowering downhole) and support, which should prove

significant for the long waveguide segments required to drill a 10 km borehole. MW-scale gyrotrons will operate at about 50% efficiency, so a cooling subsystem is needed to accommodate the 50% of heat rejected.

Real-time, downhole measurements while drilling can be recorded through remote diagnostics: these diagnostics are collinear with the MMW beam in the waveguide and operate in the MMW-Terahertz spectrum, providing *logging-while-drilling* capabilities for certain parameters. These include radiometric methods for measuring temperature and emissivity from thermal emission measurements; radar to record position/standoff distance of the waveguide and observed drilling rates, and spectroscopy for real-time chemical analysis of exhaust (Woskov & Sundaram, 2002) (Woskov & Michael, 2012). Diagnostics are also incorporated at the wellhead to measure flow rates, pressures, and temperatures at the surface, both in the waveguide and the annulus.

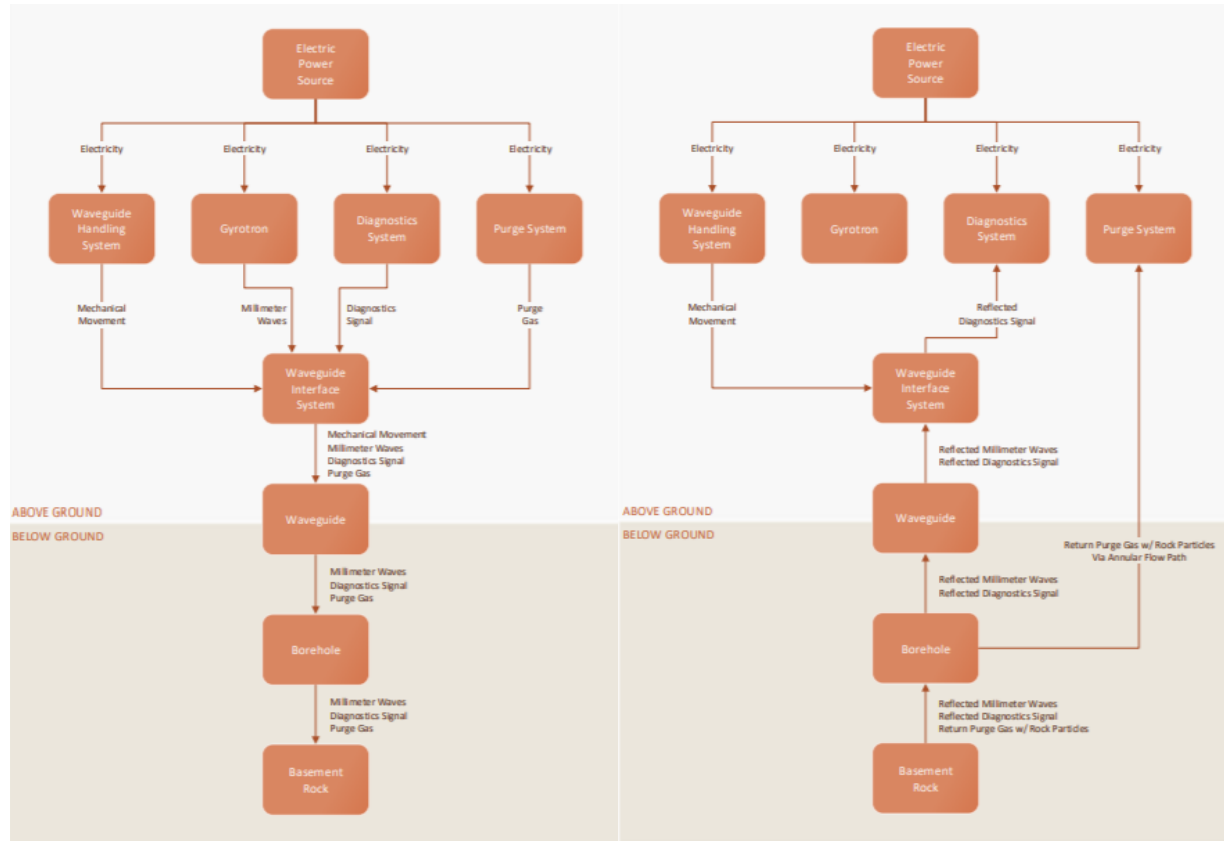


Figure 3: System Schematic. Left image is power flow delivered to borehole bottom; right image is return flow to surface

3.3 Lab Experiments

Previous experiments were performed at the MIT Plasma Science and Fusion Center with a 10 kW, 28 GHz gyrotron system in the lab. Granite and basalt were readily melted by exposure to an available incident power of 4.5 kW, raising the surface temperature to 2,000 °C - 3,000 °C within 2-3 minutes of exposure time (Woskov et al., 2014). Vitrified boreholes ranging from 20 to 50 mm in diameter and over 30 mm in depth were produced (figure 4 below). Full vaporization was not attained because experiments were limited by the maximum power available and the diffraction limits for MMW at a lower frequency. However, fundamental features of the MMW drilling system were demonstrated. These include MMW beam propagation and vitrification in a small borehole; reflected power isolation to mitigate reflected power that is not absorbed by the rock surface; waveguide-directed gas purge flow, to control plasma breakdown; and collinear combination of real-time diagnostics on the high power MMW beam (Woskov et al., 2014). The emissivity of rock was also observed to be about 30%, confirming that rock will be an efficient absorber (70%) of MMW energy.

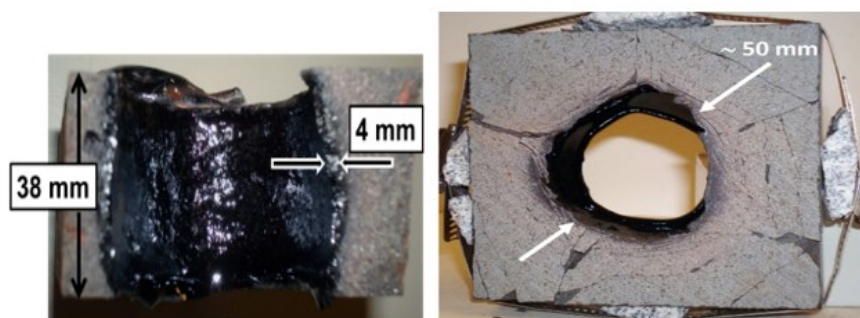


Figure 4 Experimental results to exposing a small sample of basalt to a 3-5 kW MMW beam: (left) cross-section showing vitrified liner, (right) top-view of 50-mm diameter borehole

4. PRELIMINARY CALCULATIONS

To demonstrate feasibility of a MMW drilling rig, “first principles” calculations are presented in this section that represent the fundamental physics, to demonstrate what’s possible with MMW drilling. Table 1 lists drilling parameters that will remain constant throughout each calculation, unless otherwise noted. The target ROP is 1 mm/s (3.6 m/hr), which will be sufficient to drill a 10 km deep borehole within 100 days. We anticipate this will require a 2 MW Gyrotron and a 5-1/2” waveguide.

Table 1: Drilling Parameters		
Borehole Depth, D	10	km
Borehole Diameter, $d_{b,i}$	8	inches
Target ROP	3.6	m/hr
Waveguide Outer Diameter, $d_{w,i}$	5.5	inches
Waveguide Inner Diameter, $d_{w,o}$	4.5	inches
Waveguide Density, ρ_w	8,000	kg/m ³
¹ Waveguide Yield Strength, σ_y	80	Ksi

¹ High-strength (HY-80) Steel

4.1 ROP calculation

ROP for directed energy methods can be estimated on a thermodynamic basis with melting and vaporization parameters, using equation (1) developed by Maurer (Maurer, 1968) (Maurer, 1980). The total energy required to melt and vaporize rocks can be estimated by calculating the sum of energies required to heat the solid rock to the melting point, plus the required latent heat of fusion to transform the solid to molten phase, followed by the energy needed to heat melt to the vaporization point, and finally the latent heat of energy required to transform the melt to vapor phase.

$$H = c_s(T_m - T_i) + H_f + c_m(T_v - T_m) + H_v \quad (1)$$

Updating the original data provided by Maurer, melting and vaporization parameters can serve as inputs for equation 1 to calculate the theoretical specific energies (S.E.) required to melt and vaporize a given rock composition, shown in Table 2 (Woskov & Cohn, 2009).

Table 2: Estimated Energy to Melt and Vaporize Rocks		
Rock Composition	Total Heat of Fusion (Melting) from 20 °C	Total Heat of Vaporization
	(kJ/cm ³)	(kJ/cm ³)
Granite	4.3 - 4.4	25.7 – 28.4
Basalt	4.0 - 4.8	24.7 – 27.5
Sandstone	4.5	18.7 – 19.9
Limestone	11.0	30.9 – 33.4

Now that the specific energy required to melt/vaporize a certain rock type has been determined, the rate of penetration (ROP) by way of direct energy drilling can be estimated for an absorbed power density (P.D.), which is a function of power input and the desired borehole diameter. Thus, ROP is a function of power density and specific energy required to melt/vaporize the rock.

$$ROP \left[\frac{cm}{s} \right] = (P.D. \left[\frac{kW}{cm^2} \right]) / (S.E. \left[\frac{kJ}{cm^3} \right]) \quad (2)$$

Equation 2 is plotted in figure 5 over various power inputs and borehole diameters to melt/vaporize rock with a specific energy of 26 kJ/m³, representative of granite and basalt (Woskov & Cohn, 2009). Note that the emissivity of rock has been determined in the lab to be 0.3, so roughly 70% of forward power from the gyrotron will be absorbed by the rock. For a 2 MW gyrotron, an 8” diameter borehole could be drilled through granite at an ROP of 4.4 m/hr (15 ft/hr) by full bore vaporization; ROP would increase to over 25 m/hr for the same power level if the rock is drilled by partial melt displacement. If power input and diameter are increased, a 15” borehole could be penetrated by vaporization at 80 m/hr (262 ft/hr) with 10 MW of power, or 2.5 MW through melt displacement.

Predicted ROP increases by an order of magnitude increase over rates observed in prior EGS drilling campaigns, which range from 0.4 – 2.1 m/hr (Cuniff & Bowers, 2003) (Cooper Basin, 2009) (Rischuller, 1990) (Balamir et al., 2018). Most important, ROP will not degrade significantly at higher pressures and temperatures present in the deep borehole environment so ROP should stay nearly constant with depth. Equation 2 and figure 5 represent an ideal scenario: losses throughout the borehole, waveguide, and transmission line interface will decrease these estimates considerably. However, figure 5 does show that ROP of 4 m/hr is practical: a MMW drilling operation with a constant ROP of 4 m/hr could penetrate a 10 km deep borehole within 100 days with minimal non-drilling

time, which is in line with drilling schedules for O&G and geothermal wells that are much shallower. Going forward, a target ROP of 1 mm/s (3.6 m/hr) will serve as a benchmark for later calculations.

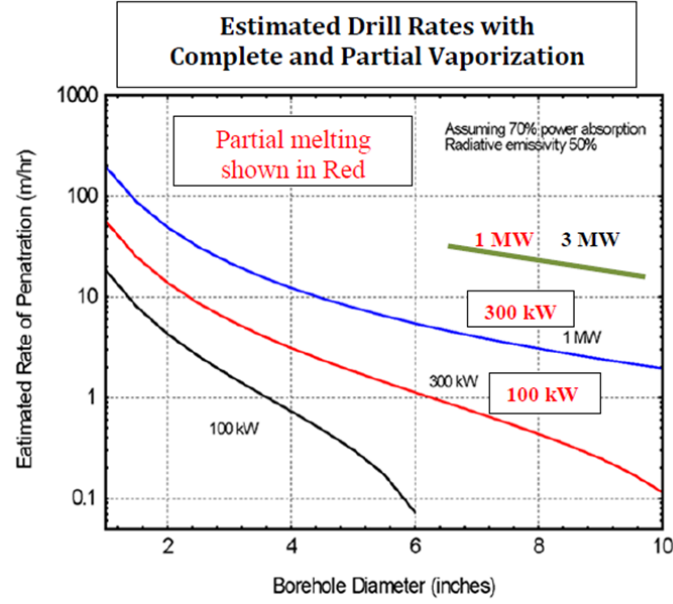


Figure 5: Estimated ROP for MMW Drilling, as a function of power input and borehole diameter. Note: power input for vaporization in black font, power input for partial melt displacement in red font (Woskov & Cohn 2009).

4.2 Material removal calculation

It is critical for all drilling operations that debris can be removed from the bottom of the borehole: MMW drilling assembly accomplishes this with the purge system, which removes both rock particles and heat during the drilling process. For full bore vaporization, the “smoke” (rock nanoparticulate) must be removed at sufficient flow velocities that exceed the terminal velocities of each rock particle; we estimate that nanoparticulate should not exceed one micrometer in diameter, so the velocity of the injected purge fluid must exceed 1.28 m/s to convey upward flow.

The mass flow rate of rock removal is a simple calculation. Using a baseline ROP of 3.6 m/hr, the mass flow rate can be calculated with density of the rock (assumed at 2,500 kg/m³ for granite). Under these assumptions, the mass flow rate comes out to 300 kg/hr.

$$\dot{m}_{rock} = \frac{\pi}{4} * d_{b,i}^2 * ROP * \rho_{rock} \quad (3)$$

4.2.1 Removal by full bore vaporization

The purge parameters are highly sensitive to fluid properties and dimensions of the waveguide/borehole, so we performed a limit analysis to identify minimum/maximum bounds for the purge gas flow rates and pressure drops. The gas flow rate must exceed the mass flow rate of nanoparticle smoke to dilute rock particulate for conveyance up-hole and to remove excess heat from downhole. This requires a multiplier, X , that is ultimately constrained by the need to remove the heat from the downhole environment to protect downhole metal components (waveguide). We have estimated a maximum value of 26.5 would be required in the worst-case scenario. The flow rates generated within the waveguide and the borehole annulus are calculated with equations 4 and 5.

$$u_{f,w} = \frac{X \rho_r d_{b,i}^2 ROP}{\rho_f d_{w,i}^2} \quad (4)$$

$$u_{f,b} = \frac{X \rho_r d_{b,i}^2 ROP}{\rho_f (d_{b,i}^2 - d_{w,o}^2)} \quad (5)$$

Maximum flow rates are predicted to occasionally exceed 100 m/s (see table 3) under a “worst-case scenario”, but this was driven by the need to remove excess heat from the borehole. These maximum limits are unlikely to exist in practice given that multiple parameters are unlikely to exist at their most extreme values simultaneously, which implies that this limit analysis requires more refinement for better accuracy. Most flow rates were bounded between 1 m/s and 100 m/s: if the multiplier was only constrained by the need to convey rock particles up-hole then flow rates for the purge gas should not exceed 65 m/s, so flow rate can be significantly reduced if a cooling component were included with the waveguide. For example, a relatively small flow of circulating cooling water, delivered by a concentric tubular downhole, could significantly decrease the expected heat transfer across the waveguide.

The purge gas will experience a significant pressure drop as it flows down through the waveguide and conveyed up-hole through the annulus with nanoparticulate smoke. These pressure drops are determined by the flow rates generated with equations 4 and 5, along with dimensions of the borehole and waveguide. Equations 6 and 7 predict the pressure drops generated within the waveguide and borehole annulus (Darcy-Weisbach equation for turbulent flow in a pipe).

$$\Delta p_{c,w} = \left(-1.8 \log \left(\left(\frac{\varepsilon_c / d_{w,i}}{3.7} \right)^{1.11} + \frac{6.9 \mu_f}{\rho_f u_{f,w} d_{w,i}} \right) \right)^{-2} \frac{\rho_f u_{f,w}^2 l_c}{2 d_{w,i}} \quad (6)$$

$$\Delta p_{c,b} = \left(-1.8 \log \left(\left(\frac{\varepsilon_c / (d_{b,i} - d_{w,o})}{3.7} \right)^{1.11} + \frac{6.9 \mu_f}{\rho_f u_{f,b} (d_{b,i} - d_{w,o})} \right) \right)^{-2} \frac{\rho_f u_{f,b}^2 l_c}{2 d_{b,i} - d_{w,o}} \quad (7)$$

In a worst-case scenario the pressure drop could exceed 100 MPa, due to the large flow rates required to remove excess heat from the downhole system (see table 3 for purge gas limits). These pressure drops are highly impractical, as the pumping power required alone would be prohibitively expensive and outside the limits of available pumping technology. However, these maximum limits are also unlikely to occur in practice, and the wide range in pressure drop implies much lower pressure drops in realistic conditions. Regardless, high flow rates and pressure drops could be required to remove excess heat from the borehole and this issue must be addressed for full-scale operating conditions.

Table 3: Limits for Purge Gas Parameters

Parameter	Nomenclature	Minimum limit	Maximum limit	Units
Pressure Drop (waveguide)	$\Delta p_{c,w}$	0.0007	82.50	MPa
Purge Velocity (waveguide)	$u_{f,w}$	0.153	841	m/s
Pressure Drop (borehole annulus)	$\Delta p_{c,b}$	0.0013	123	MPa
Purge Velocity (borehole annulus)	$u_{f,b}$	0.09	327	m/s

4.2.2 Removal by partial melt displacement

Rock melt can be permeated into the surrounding rock, provided there is enough pressure generated downhole to “push” the rock melt into low permeability granite. The drilling process will generate a volumetric rate of rock melt generated (equation 8), based on ROP.

$$q_{melt} = \frac{\pi}{4} * d_{b,i} * ROP \quad (8)$$

We assume half of the melt flow makes up the 1” thick vitrified wall along the 8” diameter BH, $d_{b,i} = 8$ ”; the remaining half must be displaced into the in-situ granite for removal, or $d_{melt} = 10$ ”. Assuming a liner thickness of 1” (see section 4.3); liquid viscosity of 4 poise for the granite melt, ν_{melt} ; and the permeability of thermally-cracked granite, k equal to 10^{-14} m^2 ; then the downhole pressure gradient required to displace granitic melt into the surrounding formation is expressed by equation 9, which comes out to 900 MPa.

$$\Delta p_{melt} = \frac{1}{16} * (\nu_{melt}) / (k) * (d_{b,i}) / (t) * ROP * \ln(d_{melt} / d_{b,i}) \quad (9)$$

900 MPa is within bounds of the overpressure condition (1000 MPa) estimated as a result of high-temperature drilling operation, but in-situ granite will have a permeability closer to 10^{-18} m^2 , three orders of magnitude higher. We are assuming that cracking due to thermal stresses and the overpressure will enhance permeability by nearly 4 orders of magnitude. Thermally induced microfractures will only increase porosity by a few percent, but a small percent change in porosity could increase permeability by 7 orders of magnitude or more (Meredith et al., 2012). Therefore, our assumption is within bounds for temporary permeability enhancement due to thermal cracking but must be demonstrated experimentally in later testing campaigns. A more detailed analysis would incorporate a dynamic, multi-physics (geomechanics, heat transfer, fluid mechanics) simulation of the melt displacement process to identify proper limits for permeability enhancement and pressure gradient required to permeate melt into in-situ granite.

4.3 Liner strength calculation

The formation of a vitrified borehole liner by rock melting penetration was first demonstrated in the Los Alamos Subterrene project (Altseimer et al., 1976). Glass melt has proven to be more competent than an unlined open borehole and should also serve as an ideal conduit for high temperature corrosive geothermal fluids, which would damage conventional steel + cement casing (Rowley & Neudecker, 1985). Casing could range up to 50%-70% of total well costs if a specialty alloy like titanium casing is required to mitigate corrosion (GEECO, 2011).

The vitrified liner will require a certain thickness to prevent wellbore collapse. Glass can have a compressive strength of 1000 MPa (Physical Properties of Glass). At 10 km depth, we can expect a lithostatic pressure of 250 MPa downhole for granite (density = 2500 kg/m^3). The wellbore will experience a compressive hoop stress, and failure (borehole collapse) occurs when the borehole hoop stress exceeds the compressive strength of the glass.

$$\sigma_{c,b} = \frac{P_{lith} * d_{b,i}}{2t} \quad (10)$$

Solving equation 10 for thickness with assuming an 8” diameter borehole, we find that the vitrified wall only needs to be 1” thick to prevent borehole collapse, all the way down to 10 km.

4.4 Rig structure calculation

Monobore capability will be constrained by the yield strength of the waveguide, which could fail under its own weight at km-length pipe segments. The waveguide will fail when the axial stress (i.e. weight) exceeds the yield strength of waveguide material (steel).

$$\sigma_{y,w} = L * \rho_w * g \quad (11)$$

Using the waveguide parameters given in table 1 and solving equation 11 for length of waveguide, L, results in a maximum length of 7 km before the waveguide should yield under its own weight. To exceed 7 km, waveguide segments must be suspended under a waveguide with larger diameter up-hole, like the “telescope” geometry used in conventional casing programs.

If a 10 km long, telescoping waveguide can be fabricated, then we can determine the strength and power rating of “drilling rig” required to support the waveguide assembly. Assuming a safety factor of 2, the weight rating can be calculated with equation 12 which comes out to 900 tons-force for the rig’s weight rating: a 1000-ton rig will be required.

$$R = 2 * \text{weight rating} = \frac{\pi}{2} * (d_{w,o}^2 - d_{w,i}^2) * L * \rho_w * g \quad (12)$$

The minimum power rating for the rig must support and convey the waveguide at 1 m/s when the waveguide is being raised or lowered. Equation 13 yields a power rating of 5,300 horsepower (HP), which is large but within range of operational drilling rigs.

$$P_{rig} (\text{power rating}) = w * v_w = \frac{\pi}{2} * (d_{w,o}^2 - d_{w,i}^2) * L * \rho * g * v_w \quad (13)$$

5. COST MODEL

A techno-economic analysis for MMW drilling operation was previously conducted by MIT and Impact Technologies, using the US Air Force 2 MW, 95 GHz gyrotron system as a reference (Oglesby et al, 2014). Estimates for capital and operational expenses are broken down in the tables below, extrapolated to a 10 km deep, 8” diameter hole section. Capital costs include the gyrotron tube, magnet, and Mirror Optics Unit (MOU) assembly; downhole waveguide and piping; purge injection subsystem, with compressors and electric generator; and the MMW-specific rig structure, including the wellhead manifold as well as cooling and controls subsystems for the gyrotron (CPI 2018). The total capital cost for the MMW drilling rig comes out to \$21.3M, or \$213k per well if amortized over a 100 well lifetime for the rig. However, our approach would retrofit a conventional rig with hybrid MMW drilling capability, so the total capital cost should also factor in the cost of a conventional drill rig, estimated at \$100M-\$150M (including expenses to retrofit for MMW drilling capability). Total capital costs now equal \$171.3M, so clearly the MMW components only make up 10-20% of the total rig cost. The operational costs depend on the price of electricity, the only consumable required for operation (purge gas will be cooled, treated, and recycled). To drill a 10 km deep well with 2 MW in 100 days requires 11,111 MWh of electricity. Assuming \$0.1/kWh for the price of electricity yields an operational cost of \$1.11M. Combining capital and operational expenses, we predict the total cost of drilling a 10 km well with MMW comes out to \$2.82M, or \$282.4/m. Note these are drilling-only costs for MMW; as explained below, we will complement MMW drilling through basement rock to target depth with a conventional drilling operation from the surface to the basement rock contact, which will raise total well costs significantly.

Table 5: Cost to drill a full-sized well (10 km, 8” diameter) MMW		
Unit	Cost (\$ million USD)	Notes
Capital Costs		
2 MW Gyrotron	\$2.5M	2-MW tube, magnet, MOU assembly, and diamond window
Downhole piping/waveguide	\$3.28M	Estimated (\$100/ft)
MMW Rig structure	\$8M	Includes wellhead manifold and tools; controls and heat exchanger subsystems for gyrotron
Purge system	\$7.5M	High-powered compressors with gas supply and generator
Conventional rig	\$150M	Cost assumption: Drilling rate of \$15,000/day * 100 days, amortized over 100 wells. Also includes cost to retrofit rig for compatibility with hybrid MMW operation
Total Capital Cost	\$171.3M	
Capital Costs (per well)	\$1.71M	Amortized over 100 wells drilled.
Operating Costs		
Electricity Costs	\$1.11M	10 km deep well, w/ ROP = 4 m/hr and electricity cost \$0.1/kWh
Total cost (per well)	\$2.82M	
MMW Drilling Costs	\$282.4/m	Conventional: \$1,000/m - \$4,000/m

Few wells have been drilled past 10 km, but deep EGS wells drilled to an average depth of 5 km range from \$1,000/m to \$4,000/m, so MMW drilling can reduce drilling costs 10-fold (Tester et al., 2006). Savings are representative of ROP improvement; absence of casing costs, replaced by the vitrified liner to stabilize/support the borehole; and reducing the number of casing strings. Partial melt displacement could increase the ROP five-fold, dropping the total cost to roughly \$1.9M (\$190/m) per well.

MMW drilling can greatly improve the economics of supercritical EGS anywhere due to lower well costs, despite the large depths drilled. AltaRock has developed a model to calculate the Levelized Cost of Electricity (LCOE) for supercritical EGS, based off the techniques used in the GETEM tool but modified for supercritical temperatures (Claudohos et al., 2018). Extrapolating drilling costs to 10-20 km depths is impractical, but the Newberry reference used in the AltaRock model serves as a useful comparison. The Newberry site contains a shallow heat source where supercritical temperatures are encountered near 4.5 km depth. Total well costs came out to roughly \$28M per well, which included \$10M in drilling-only costs and \$10M in casing costs with an expensive high-temperature alloy like titanium, which could range up to \$3,000/m (Finger & Blankenship, 2010). The overall LCOE for supercritical EGS at the Newberry site is just over \$50/MWh, which can be competitive with other alternative energy sources including wind, solar, and advanced nuclear (EIA, 2019). Now, let's replace the shallow well with a 20 km well drilled with MMW; this represents a conservative depth target that would reach supercritical temperatures at most locations. We assume the first 2 km are drilled conventional (\$3,500/m, with high-temperature casing included), and the next 18 km are drilled with MMW. Total well costs for the 20 km well would come out to \$23M per well, which results in an LCOE of \$49/MWh. The LCOE is equivalent to the Newberry reference case, validating the case for supercritical EGS to be competitive at 10-20 km depth anywhere with MMW drilling. Developmental risk costs would also be avoided since supercritical EGS targets can always be reached if the well is drilled to a deeper depth, although this was not factored into the LCOE calculation.

6. DEVELOPMENT ROADMAP

A development roadmap for MMW drilling is provided in table 6, along with the Technology Readiness Level (TRL) anticipated for each development milestone, which is measured by aspect ratio (Borehole Length : Borehole Diameter).

Table 6: Technology Development Roadmap						
Deep Drilling TRL	TRL 3	TRL 4	TRL 5	TRL 6	TRL 7	TRL 8
Aspect Ratio (Length:Diameter)	1:1	10:1	100:1	1000:1	1,000:1	50,000:1
Dimensions (depth, diameter)	5 cm x 2"	50 cm x 2"	5 m x 2"	100 m x 2"	1 km x 4"	10 km x 8"
Power input	10 kW	100 kW	100 kW	500 kW	500 kW	1 MW
Frequency (GHz)	28	95	95	50-300	50-300	50-300
Operational time	1-10 minute	10-100 minutes	10-100 minutes	1-10 days	1-10 days	100 days
Purge: Flow Rates (m ³ /s)	NA	0.001-0.01 (air)	0.01-0.1 (air)	0.01-0.1 (air)	0.1-1 (gas)	0.1-1 (gas)
Pressure (MPa)	NA	0.1-1	1-10	1-10	10-300	10-300
Material Removed (m ³)	NA	0.001	0.01-1	0.01-1	10-300	10-300
Waveguide dimensions	1 m long, 1.5" diameter	1-5 m long, 1.5" diameter	5-20 m long, 1.5" diameter	10-1000 m long, 3" diameter	10-1000 m long, 3" diameter	1000-10000 m long, 6" diameter
Waveguide Weight Rating	200 kg	200 kg	200 kg	20,000 kg	20,000 kg	1,000,000 kg
Wellhead Pressure Isolation	NA	1 MPa	1 MPa	100 MPa	100 MPa	300 MPa

As noted earlier, previous lab experiments were limited by the power input and low frequency for effectively penetrating boreholes, which did not breach 50 mm depth. The next steps for experimentation and field testing follow the roadmap outlined in table 6 above. Increasing the power level and frequency to 100 kW and 95 GHz, respectively, will enable drilling a 100:1 borehole (20-m long, 2" diameter) above ground, which will prove material removal can be achieved over extended distances and pressures isolated at the wellhead/away from the gyrotron. Then a MW scale gyrotron and subsystems must be acquired for the next stage of development: this stage will incorporate a prototype "MMW drilling rig" that initially can drill shallow subsurface boreholes. It is necessary that the prototype demonstrate compatibility with a conventional drilling rig, the steps outlined above will all be accompanied by a modelling and simulation campaign focused on modelling the multi-physics behavior of energy-rock interaction, to justify next steps in lab and field testing.

Once fundamentals are demonstrated at larger aspect ratios at the surface, the next steps will steadily increase power/length/diameter drilled to approach deep boreholes. Technology developments required to enable deep drilling include a MW-scale MMW reflected power isolator, high-pressure windows and a pressure management scheme to mitigate the higher pressures generated downhole, and a waveguide fill transparent to MMW at supercritical conditions (high pressures) representative of the deep borehole environment. A final product would incorporate all components into a transportable “drilling rig” that can be combined with conventional drilling equipment for a hybrid operation. Conventional drilling will be used to breach through the upper layer of sedimentary rock and unconsolidated sediments, until basement rock is reached. Then MMW drilling operation takes over and drills to the predicted depth target for supercritical temperatures.

The development timeline for supercritical EGS will take several years, so MMW technology will enter into first markets unrelated to geothermal energy. MMW technology is widely applicable to industries that incorporate rock destruction methods (tunnel boring, mining, trenching, construction). An above-ground drilling demonstration will prove MMW technology in the field and serve as a basis to license MMW technology, as a near-surface *rock-weakening/destruction product*, for non-energy related industries, so that our team can still focus on geothermal energy while operations experiences is acquired. For subsurface drilling, the first market could be drilling exploratory boreholes for shallow geothermal resources (conventional or low-T EGS), with a small MMW drilling rig prototype. Once the prototype is proven at shallow depths, we will then progress development to deeper and larger boreholes until a 10 km can be demonstrated by the MMW drilling rig.

CONCLUSION

Supercritical EGS is the only renewable, dispatchable energy source that approaches the power densities required to replace fossil fuels for a full global low-carbon energy transition. MMW drilling can enable a supercritical EGS well anywhere on the planet, allowing geothermal to scale as a significant source of energy to the world. MMW directed energy will vastly improve deep drilling with conventional methods: no mechanical systems in the wellbore that could wear out or break, no limit on temperature exists, penetration rates will become marginally more difficult with depth and harder rock, and casing could be replaced by a durable vitrified liner. MMW drilling could make the economics of a 20 km deep, supercritical EGS well competitive with any available energy resource, which can position geothermal energy as the leading technology for reducing greenhouse gas emissions.

NOMENCLATURE

H	Total Energy required to melt or vaporize rock (J)
c_s	Mean Heat Capacity of Solid (J/g/K)
T_i	Initial Temperature (°C)
T_m	Melting Temperature (°C)
H_f	Latent Heat of Fusion (J/g)
c_m	Mean Heat Capacity of Melt (J/g/K)
T_v	Vaporization Temperature for 1-3 atm (°C)
ROP	Rate of Penetration (m/s)
$P.D.$	Power Density (kw/cm ³)
$S.E.$	Specific Energy (kJ/cm ³)
\dot{m}_{rock}	Mass Flow rate (kg/hr)
ρ_{rock}	Rock Density (kg/m ³)
$d_{w,i}$	Inner Diameter of Waveguide (inches)
$d_{w,o}$	Outer Diameter of Waveguide (inches)
$d_{b,i}$	Inner Diameter of Borehole (inches)
d_{melt}	Diameter of melt extruded into in-situ rock (inches)
X	Dilution Multiplier
$u_{f,w}$	Flow Rate in Waveguide (m/s)
$u_{f,b}$	Flow Rate in Borehole Annulus (m/s)
$\Delta p_{c,w}$	Pressure drop within Waveguide (MPa)
$\Delta p_{c,b}$	Pressure drop within Borehole Annulus (MPa)
L, l_c	Length of Waveguide (m)

ε_c	Surface Roughness of Waveguide, Borehole
$\sigma_{c,b}$	Hoop stress of Borehole (MPa)
p_{lith}	Lithostatic Pressure (MPa)
q_{melt}	Volumetric flow rate of liquid melt (m ³ /s)
ν_{melt}	Viscosity of liquid melt, granite (Poise)
k	Permeability of in-situ granite (m ²)
Δp_{melt}	Pressure gradient required to permeate granite melt through in-situ rock (MPa)
t	vitrified liner thickness (inches)
$\sigma_{y,w}$	Waveguide Yield Strength (MPa)
ρ_w	Waveguide Density (kg/m ³)
P_{rig}	Rig Power Rating (HP)
v_w	Waveguide Velocity (m/s)

REFERENCES

- Altseimer, J.H. et al.: The Subterrene Rock-Melting Concept Applied to the Production of Deep Geothermal Wells, *Los Alamos National Lab* (1976), LA-UR-76-1302, Q-23.
- Balamir, O., Rivas, E., Rickard, W.M., McLennan, J., Mann, M., and Moore, J.: Utah FORGE Reservoir: Drilling Results of Deep Characterization and Monitoring Well 58-32, *Proceedings, 43rd Workshop on Geothermal Reservoir Engineering*, Stanford University, Stanford, CA (2018).
- Blank, M., Borchard, P., Cahalan, P., Cauffman, S., Felch, K., and Jory, H.: Development and Demonstration of a Multi-Megawatt 95 GHz Gyrotron Oscillator, *35th IEEE Conf. on Plasma Sci.*, Karlsruhe, Germany, (2008), IEEE 978-1-4244-1930-2/08.
- CPI (Communications and Power Industries, Inc.): Private Communication (2018).
- Cooper Basin Project Updates, ASX Announcements, Dec 2008 – Jan 2009, *Geodynamics* (2009).
- Cunniff, R.A., and Browers, R.L.: Final Report Enhanced Geothermal Systems Technology, Phase II, *U.S. DOE*, DE-FC07-011D14203, (2003).
- Dobson, P., Asanuma, H., Huenges, E., Oletto, F., Reinsch, T. and Sanjuan, B.: . Supercritical Geothermal Systems – a Review of Past Studies and Ongoing Research Activities, *Proceedings, 41st Workshop on Geothermal Reservoir Engineering*, Stanford University, Stanford, CA (2017).
- DOE (U.S. Department of Energy): Geovision Harnessing the Heat Beneath our Feet, *DOE*, Washington, D.C., (2019), ch. 3, p. 59.
- EIA (U.S. Energy Information Administration): Levelized Cost and Levelized Avoided Cost of New Generation Resources in the Annual Energy Outlook 2019, *DOE*, Washington, D.C. (2017).
- EIA (U.S. Energy Information Administration): International Energy Outlook Executive Summary, *DOE*, Washington, D.C. (2017).
- Finger, J. and Blankenship, D.: Handbook of Best Practices for Geothermal Drilling, *Sandia National Laboratories*, (2010), p. 28.
- Friðleifsson, G.Ó., Elders, W.A., and Albertsson, A.: The concept of the Iceland Deep Drilling Project, *Geothermics* (2014).
- Gahan, B.G.: Processing Rock, *Indust. Laser Solutions*, (Sep 2005), pp. 16-18.
- GEECO (Gas Equipment Engineering Corporation): Baseline System Costs for a 50MW Enhanced Geothermal System, *DOE DE-EE0002742-002*, preliminary report, (March 2011).
- Hagen, K.D.: Heat Transfer with Applications, *Prentice-Hall, Inc.*, (1999) Eq. 5-10, p.171 and Appendix D, rock thermal properties
- Hunten, D.M., Turco, R.P., and Toon, O.B: Smoke and Dust Particles of Meteoric Origin in the Mesosphere and Stratosphere, *J. of Atmospheric Sci.*, (1980) vol. 38, 1342-1357.
- Jacquiot, J.: Plasma heating and current drive systems for ITER and Future Fusion Devices, *17th IEEE/NPSS Symposium Fusion Engineering* (1998), Cat. No.97CH36131, vol.1, pp. 399-404.

- Jung, R.: EGS – Goodbye or Back to the Future, *Proceedings of the International Conference for Effective and Sustainable Hydraulic Fracturing*, Brisbane, Australia, (May 2013), ch. 5, pp. 95-121
- Lowry, T.S., Foris, A., Finger, J.T., Pye, S., and Blankenship, D.A.: Implications of Drilling Technology Improvements on the Availability of Exploitable EGS Resources, *Proceedings, 42nd Workshop on Geothermal Reservoir Engineering*, Stanford University, Stanford, CA, (2017).
- Maurer, W.C.: Novel Drilling Techniques, *Pergamon Press*, London, (1968) pp. 87-91.
- Maurer, W.C. : Advanced Drilling Techniques. *Petroleum Publishing Co.*, (1980), ch. 17.
- Meredith, P. G., Main, I. G., Clint, O. C. & Li, L.: On the threshold of flow in a tight natural rock. *Geophysical Research Letters*, (2012), vol. 39, issue 4.
- Nikolaevskiy, V. and Garagash, I.: Earth Crust Structure as a Result of Rock Fracturing at High Pressure and Temperature Conditions, *Coupled Thermo-Hydro-Mechanical Chemical Processes in Geo-Systems* (2002).
- Nordstrom, D.K. and Munoz, J.L.: Geochemical Thermodynamics, 2nd edition, *The Blackburn Press*, (1994) Ch. 1.
- Nusinovich, G.S.: Introduction to the Physics of Gyrotrons, *John Hopkins Studies in Applied Physics* (2004).
- Nusinovich, G.S., Thumm, M.A., and Petelin, M.I.: *J. Infrared Milli Terahz Waves*, (2014), vol. 35 pp.325-381.
- Oglesby, K.D., Woskov, P.P., Einstein, H.H., and Livesay, B.: Deep Geothermal Drilling Using Millimeter Wave Technology Final Technical Research Report. *U.S. DOE Office of EERE – Geothermal Technologies Program*, (2014), pp. 15-16.
- Physical Properties of Glass. *Saint Gobain Building Glass UK*.
- Rischuller, H.: Example for Advanced Drilling Technology, *Oil Gas* 16 (1990), no. 4, 16-20.
- Rowley, J.C. and Neudecker, J.W.: In-Situ Rock Melting Applied to Lunar Base Construction and for Exploration Drilling and Coring on the Moon. *Conference: Lunar Bases and Space Activities of the 1st Century*, Washington, D.C., (1984), pp. 465-477.
- Tester et al.: The Future of Geothermal Energy, *MIT*, (2006), Fig. 1.8.
- WEC (World Energy Council): World Energy Resources: Geothermal, *World Energy Council 2013*, (2013), 9.2.
- Whitlock, R.D. and Frick, G.M.: Particle size distributions of aerosols formed by laser ablation of solids at 760 Torr, *J. Mater. Res.*, (1994), vol. 9, 2868-2872.
- Woskov, P.P. and Cohn, D.R. (2008). *US Patent # 8,393,410 B2: Millimeter-Wave Drilling System for Gas, Oil and Geothermal energy*.
- Woskov, P.P., and Cohn, D.R.: Annual Report 2009 Millimeter Wave Deep Drilling for Geothermal Energy, Natural Gas and Oil, *MIT Plasma Science and Fusion Center, Report PSFC/ RR-09-11*, Cambridge, MA (2009).
- Woskov, P.P., Einstein, H.H., and Oglesby, K.D.: (2014). Penetrating rock with intense millimeter-waves. 1-2. 10.1109 IRMMW-THz 2014 (2014), 1-2.
- Woskov, P.P., and Michael, P.: Millimeter-Wave Heating, Radiometry, and Calorimetry of Granite Rock to Vaporization, *2013 IEEE MTT-S International*, Seattle, WA, (June 2013), 2-7.
- Woskov, P.P. and Sundaram, S.K.: Thermal Return Reflection Method for Resolving Emissivity and Temperature in Radiometric Measurements, *MIT Plasma Science and Fusion Center*, Cambridge, MA (2002).
- Zimmer, A.T.: The Influence of Metallurgy on the formation of aerosols, *Journal of Environmental Monitoring*, (2002), vol. 4, 628-632